HIGHLY OBLIQUE BISTATIC RADAR OBSERVATIONS USING MARS GLOBAL SURVEYOR

Richard A. Simpson

Packard Bldg - Room 332, Stanford University, Stanford, CA 94305-9515, USA
rsimpson@magellan.stanford.edu

ABSTRACT

Since 1998, we have collected over 8000 Mars Global Surveyor radio occultations more than half accompanied by transient surface echoes. These echoes arise when the spacecraft high-gain antenna (HGA) incidentally illuminates parts of the surface near the occulting limb. The 3-dB HGA beamwidth is 1.6°, so the majority of echo energy results from illumination at incidence angles $\phi>89^o$. Conventional quasi-specular scattering models are questionable at angles $\phi>60^o$. We describe our search for echo properties which may be useful in characterizing the scattering mechanism.

INTRODUCTION

Finite width of the Mars Global Surveyor (MGS) high-gain antenna (HGA) beam ensures that part of the planet's surface near the limb will be illuminated just before occultation ingress and just after occultation egress (Fig. 1). Such Mars surface echoes were first reported in 1969 at wavelength λ=13 cm and incidence angles $\phi>86^o$ during Mariner 6 and 7 flybys [1]. Mariner echo widths were interpreted based on the viewing geometry, which required local surface tilts of 1.5° for the observed 60 Hz frequency dispersion. Assumptions behind classical bistatic radar theory [2] are questionable at angles $\phi>60^o$; various measurements confirm that both large- and small-scale shadowing have significant negative impact on echoes at angles $\phi>85^o$ [3]. The fact that the MGS observing geometry is more extreme than that for the Mariners, yet surface echoes accompany more than half of over 8000 MGS occultations, means that both the scattering mechanisms and the surface properties responsible for these echoes need to be understood. The surface information in these echoes is potentially a useful byproduct of the atmospheric occultation data collection.

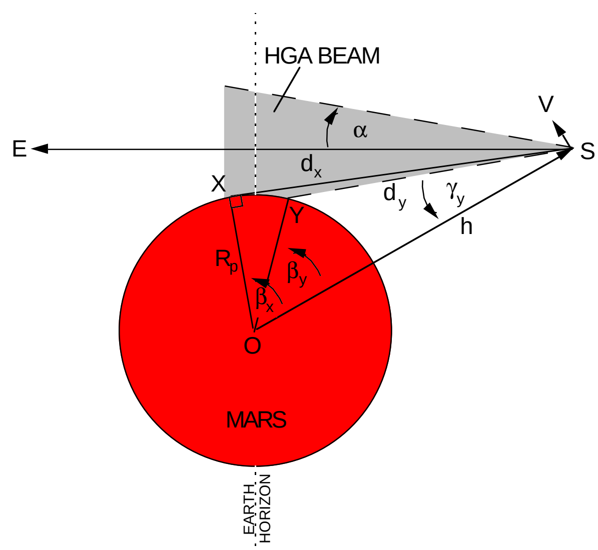

Fig. 1. While the spacecraft (S) to Earth (E) ray clears the limb during an egress occultation, the high-gain antenna beam illuminates part of the surface (shown in side view as arc XY). Only the portion of XY visible from Earth (left of the Earth Horizon line) contributes to the received echo.

Mars Global Surveyor radio science subsystem characteristics are summarized in Table 1 [4]. Ground values are for nominal operations using a 34-m diameter antenna of the NASA Deep Space Network (DSN). Infrequently, MGS has used a 70-m DSN antenna, which increases gain by 6 dB and reduces system noise temperature to 20 K. The range in carrier-to-noise ratio reflects variations over two years in Earth-Mars distance (~0.5-2.5 A.U.). Typically 8-10 occultations are captured each day; because of spacecraft limitations (not relevant to this discussion), most of those captured are ingress occultations at northern polar latitudes (~60°N). Near opposition most occultations yield detectable surface echoes; near superior conjunction most do not. But echoes have been seen at all Earth-Mars ranges.

Table 1. Mars Global Surveyor Radio Subsystem Characteristics

Parameter	**Value**
Spacecraft	
Radiated Power (continuous wave)	21 w
Antenna Boresight Gain	39.1 dBi
Antenna Beamwidth	1.6° (half-power, full width)
Frequency	8423 MHz
Ground (34 m antenna)	
Antenna Gain	68 dBi
System Noise Temperature	30 K
Carrier-to-Noise Ratio	45-60 dB/Hz

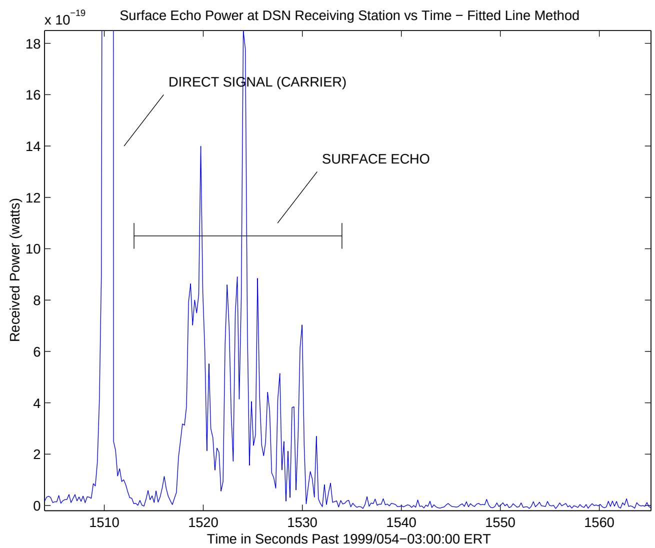

Fig. 2. Summed power in an egress echo from 1999/054. Echo is assumed to lie within 7 frequency bins centered on a best fit line to echo's time-frequency trajectory. Contribution from carrier can be large, but is easily excised. Average echo power is computed only over time when echo is within the receiver passband.

Surface echoes have distinct time-frequency signatures. During egress, for example, the surface echo diverges linearly from the directly propagating carrier at the occultation point. Echoes typically begin weak (1515 s in Fig. 2), increase in strength as more surface area is illuminated (1520-1525 s), and finally drop sharply as HGA illumination leaves the surface (1530 s). During the "growth" phase, echoes fade on time scales less than a second (constructive and destructive interference) and also longer because of changes in the scattering properties of the illuminated surface or because the surface is screened from either the spacecraft or receiver by intervening topography. For most MGS experiments, the sharp drop occurs (coincidentally) near where the signal moves out of the receiver passband. Often a weak "precursor" is visible for a few seconds while the spacecraft itself is hidden behind the limb. During ingress occultations, the sequence is reversed; the surface echo and carrier frequencies merge at the occultation point.

ANALYSIS AND INTERPRETATION

We selected observations from five months around opposition in 1999 and studied the echoes in some detail. First, we calculated echo power (relative to the carrier) as a function of time and computed an average echo power for each event. The average calculation provides a single measure of echo intensity that hides both the short- and long-term amplitude fluctuations. Second, we computed the observing geometry for each observation, including both the location of the reflecting region on Mars and the spacecraft antenna pointing. The latter is important because small HGA offsets toward or away from the surface can have dramatic effects over- or under-illuminating the surface relative to nominal pointing. Third, we attempted to correlate echo behavior with surface location.

Signal Analysis

We computed power spectra from the raw receiver samples. After locating the occultation point and determining the sense of occultation (ingress or egress), we searched the appropriate half spectrum for the next strongest signal. We fitted a straight line to those points but rejected echoes for which the fitted time-frequency trajectory slope differed by more than 2 Hz/s from a running average computed for that date. We then summed the seven frequency bins centered on the fitted line. Carrier power captured near the occultation point (e.g., near 1510 s in Fig. 2) may be excluded by disregarding points when the echo and carrier have similar frequencies. Echo power was normalized by the corresponding carrier power, and average echo power was computed over a time window that excluded contributions from the carrier and times when the echo frequency was outside the receiver passband. Typical normalized average powers were 10^{-4}; highest values were an order of magnitude larger (Fig. 3).

Fig. 3 shows echo power for ingress and egress occultations versus observation date. After day 120, egress tends to give stronger echoes. On day 110, the HGA azimuth gimbal met an unexpected obstacle, and normal operations were suspended for two weeks of diagnosis and tests. Our reconstructions show HGA pointing within 0.15^{o} of the Earth direction throughout (compared with a 0.25^{o} pointing requirement), but these surface echo measurements suggest a slight pointing bias beginning with the HGA azimuth anomaly.

Observing Geometry — Spot Size and Surface Location

Observing geometry was calculated using reconstructed spacecraft orbits. Fig. 1 shows the geometry when transient echoes can be observed. Spacecraft (S) moving at velocity V radiates a microwave beam (MGS width $2\alpha=1.6^{o}$), part of which intercepts the surface between X and Y. Echoes reach the receiver on Earth (E) from that part of XY to the left of the "Earth Horizon" line. OSX forms the angle γ_x (not shown). Three times are of interest: (1) the instant of occultation (t_{occ}), when ES is tangent to the surface at X and the area A_{vis} mutually visible to transmitter and receiver is zero; (2) the instant of last illumination (t_{end}), when Y merges with X, angle ESX equals α, and A_{vis}=0.; and (3) the time of maximum illuminated area (t_{max}), between t_{occ} and t_{end}, which we take to be when angle ESY equals α and all of XY is visible from Earth. For a simplified case with MGS in a circular orbit (h=400 km) about a spherical Mars (R_p=3400 km) and Earth in the orbit plane, the arc mutually visible to spacecraft and Earth is (see Fig. 1 for definitions):

Table 2. Mutually Visible Arc for Transient Echoes at Three Times

	t_{occ}	t_{max}	t_{end}
d_x (km)	1697.056	1697.056	1697.056
β_x (deg)	26.525	26.525	26.525
γ_x (deg)	63.475	63.475	63.475
γ_y (deg)	62.675	63.463	63.475
β_y (deg)	20.510	25.737	26.525
d_y (km)	1340.947	1650.088	1697.056
Mutually visible arc XY (km)	0.	47.761	0.

Width of the illuminated region is maximum ($W_{max} = d_x \sin 2\alpha = 47.5$ km) at t_{occ} then decreases, at first slowly then with increasing rate, toward t_{end}. Surface area contributing to the echo can be approximated by the product of the length of the mutually visible XY and the decreasing W--a line perpendicular to the Earth-MGS direction at t_{occ}, a line parallel to the Earth-MGS direction at t_{end}, and approximately a rectangle between those times with maximum area ~1000 km^2.

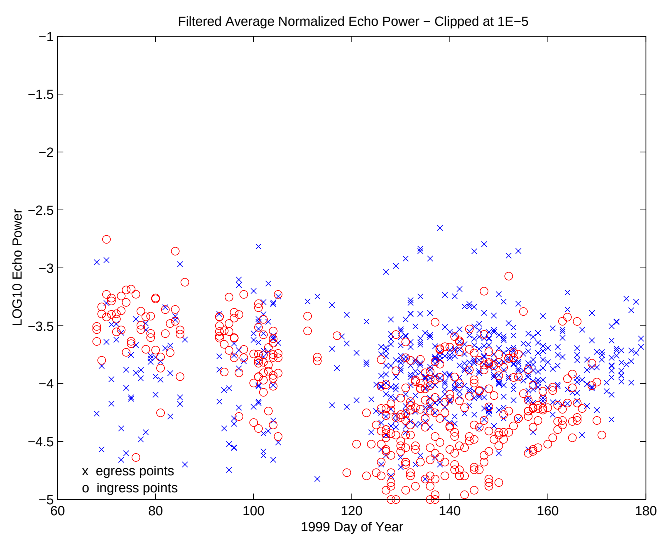

Fig. 3. Average normalized echo power as a function of observation date. Note that egress echoes generally appear weaker than ingress echoes after day 110, when an azimuth gimbal anomaly occurred.

When Earth is in the orbit plane, echo separation rate is maximum (about -37 Hz/sec) and the echo is visible for only about 30 seconds. As Earth's position moves out of the orbit plane, there are times when the viewing geometry includes no occultations (and no surface echoes). Prior to the loss of occultations, the scattering region skims along the limb, barely separated in frequency from the carrier. The non-circular nature of the orbit determines the surface covered in these cases, usually by sweeping the scattering spot in longitude while simultaneously expanding and contracting XY in latitude (as above). Table 3 shows the range of the specular point (approximately the center of the scattering region) for several cases in 1999. On 1999/068 Earth was nearly in the orbit plane and there was almost no east-west movement, but on 1999/178 the contributing region shifted nearly 200 km eastward in 50 seconds after egress.

Table 3. Specular Point Locations for Selected Occultations in 1999

Year/Day	**Orbit**	**Specular Point Start (Lat ^{o}N, ^{o}Lon E)**	**Specular Point End (Lat ^{o}N, Lon ^{o}E)**
1999/068	Nearly in plane; -37 Hz/s	(-74.7, -94.1)	(-74.0, -94.0)
1999/097	-31 Hz/s	(-73.8, -91.0)	(-73.1, -88.7)
1999/119	-19 Hz/s	(-70.7, -7.7)	(-69.8, -2.5)
1999/178	Nearly broadside; -2 Hz/s	(-67.3, 74.4)	(-66.3, 82.7)

Correlation of Echo Behavior with Location

Although a thousand echoes from 1999 were included in the study here, few of the surface scattering regions overlapped directly. The maximum 47 km diameter of the contributing spot is small compared with the total area of Mars even when the region moves, as was the case in June 1999. Egress latitudes (65-75^{o}S) were more confined than ingress latitudes (75^{o}N-20^{o}S), however, and we have examined those echoes more closely. A dozen echoes from (65-75^{o}S, 260-270^{o}E) are among the strongest and most consistent found. We have also correlated fades with presence of large-scale topography over several observations, but otherwise see nothing unusual about this area in image data.

REFERENCES

[1] G. Fjeldbo, A. Kliore, and B. Seidel, "Bistatic radar measurements of the surface of Mars with Mariner 1969," *Icarus*, vol. 16, 502-508, 1972.

[2] G. Fjeldbo, *Bistatic-Radar Methods for Studying Planetary Ionospheres and Surfaces*, Ph.D. dissertation, Stanford University, 1964.

[3] J.F. Vesecky, "Electromagnetic wave scattering from a gently undulating, rough surface at near grazing incidence," *Proceedings of the DARPA Low Angle Tracking Symposium*, vol. I, 39-62, Santa Barbara, CA: General Research Corp., 1977.

[4] G.L. Tyler, G. Balmino, D.P. Hinson, W.L. Sjogren, D.E. Smith, R.A. Simpson, S.W. Asmar, P. Priest, and J.D. Twicken, "Radio science observations with Mars Global Surveyor: orbit insertion through one Mars year in mapping orbit," *Journal of Geophysical Research,* vol. 1066, 23327-23348, 2001.